Multiple-Scale Interactions during an Extreme Rainfall Event over Southern Vietnam

Thang, V. V.[1], Thanh, C.[2] and Tuan, B. M.[2*]

1. Ph.D., Vietnam Institute of Meteorology, Hydrology and Climate Change, Hanoi, Vietnam
2. Instructor, Department of Meteorology and Climate change, Faculty of Meteorology, Hydrology and Oceanography, Hanoi University of Science, Vietnam National University, Hanoi, Vietnam

Abstract

In August 2019, southern Vietnam suffered its worst flooding to date, which was also associated with record-breaking extreme rainfall. This study seeks to explain how this extreme rainfall event can be distinguished from normal rainfall events. The bandpass filter applied to the observed rainfall shows that there were significant intensifications of 3–10-day variation and 11–60-day oscillations during the event. While the latter is characterized by the intensification of westerly flows from the Bay of Bengal to southern Vietnam, the former is related to more complex movements of a series of synoptic-scale disturbances over the western North Pacific. The notion of multiple-scale interactions, inducing the extreme rainfall event is supported by diagnosing the anomalous columnwise moisture divergence over the southern plain region of Vietnam. It is demonstrated that the anomalous convergences associated with the long-term mean moisture and the synoptic-scale moisture transported by the long-term mean flow are the most important factors for formation of the extreme rainfall event.

Keywords: Synoptic wave-train, Large-scale circulation, Intraseasonal oscillation, Moisture convergence, Extreme rainfall.

1. Introduction

The southern Vietnam is a major region contributed to the Vietnamese economy. Although the region accounts for more than 45% of the Vietnamese gross domestic product each year, it often suffers serious natural disasters related to heavy rains and flooding. The flooding is more problematic when heavy rain occurs during high tidal times, which results in water levels in rivers and canals rising higher than the sewer discharge valves and prevents discharge through the normal sewage system. Therefore, studies of the mechanism for occurrence of extreme rainfall in southern Vietnam have a critical role in mitigation of the resulting environmental and socioeconomic impacts.

According to Nguyen and Nguyen (2004), the Vietnam climate can be classified into seven sub-regions. Located in the tropics, the southern plain is characterized by a distinct climate compared to other parts of Vietnam. Due to the effect of the oceanic air masses, the temperature in southern Vietnam remains constant year-round, and its climate can be simply divided into dry and wet seasons. Characterized by less precipitation, the dry season begins in November and ends in April (Nguyen and Nguyen, 2004; Nguyen et al.,

2014). In contrast, the wet season (i.e., from May to October) is strongly modulated by the Asian summer monsoon with much more rainfall than in the dry season (Pham et al., 2010; Nguyen-Le et al., 2014; Nguyen-Thi et al., 2010). Rainfall in the wet season comes generally from short-duration showers in the mid-afternoon to early evening (Takahashi et al., 2010).

Heavy rainfall in southern Vietnam is often related to the activities of intraseasonal oscillations (ISOs) and tropical cyclones (Van der Linden et al., 2016; Tuan, 2019; Nguyen-Thi et al., 2010). Van der Linden et al. (2016) determined the phase of the Madden–Jullian oscillation (MJO) and convective coupled equatorial waves using the method proposed by Yasunaga and Mapes (2012) and found that the number of days with observed rainfall greater than 25 mm day^{-1} increased by approximately 50% during the wet phases of the MJO and equatorial Rossby (ER) and Kelvin waves. Van der Linden et al. (2016) observed that in the wet phase of the MJO, the depth and velocity of the westerly monsoon increases strongly, leading to strong lower-level wind shear and transport of a large amount of

moisture from the Bay of Bengal (BOB) to the southern region. These changes in tropospheric structure create strongly unstable conditions that favor the outbreak of deep convection. In the wet phase of Kelvin and ER waves, the low-level troposphere is also moistened, but the change in depth of monsoon layers and vertical wind profile are not as distinct as in the wet phase of the MJO. Tuan (2019) investigated the relationship between sub-monthly oscillations and the number of heavy rainfall days in seven climatic sub-regions. The results emphasized that during the wet phase of sub-monthly oscillation of rainfall in the southern plain, the upstream development of wave trains along the subtropical jet stream consistently enhances the cyclonic circulation of tropical-type waves over the East Sea. The tropical–extratropical interaction causes strong low-level convergence, deepening the convective activities that might cause heavy rainfall in the region. However, the relationship between the sub-monthly activities and heavy rainfall in the southern plain is not as clear as the other climatic sub-regions. Nguyen-Thi et al. (2010) studied the contribution of tropical cyclones to seasonal rainfall patterns in Vietnam and found that tropical cyclones do not significantly contribute to total annual rainfall over Southern Vietnam. The month with the most contribution of rainfall from tropical cyclones in the region is November.

During August 1–15, 2019, the southern plain, especially Phu Quoc Island, experienced the worst flooding in its history associated with heavy rainfall. On Phu Quoc Island, 8424 houses were reported as inundated, and the total damage was estimated at more than US $4.6 million (Vietnamnews, 2019). In this study, the major goal is to investigate the characteristics of large-scale patterns associated with this extreme rainfall event. The data and methods used for the analysis are described in Section 2. Section 3 discusses the evolution of large-scale patterns associated with extreme rainfall events. Finally, the conclusions of this study are given in Section 4.

2. Data and Methodology

The observed rainfall data are collected from eight rain gauges over southern Vietnam during the period from 1980 to 2019, retrieved from the Vietnam Meteorology Hydrology Administration (Figure 1). The daily PERSIANN rainfall (Nguyen et al., 2019), which is estimated from satellites, is used to analyze the spatial distribution of rainfall. The other major dataset used in this study is the daily reanalysis data provided by the National Centers for Environmental Prediction (NCEP) and the National Center for Atmospheric Research (NCAR) (Kalnay et al., 1996). In addition to the reanalysis data, the Global Precipitation Climatology Project (GPCP) product (Adler et al., 2016) was also used to address the seasonal progression of the Asian summer monsoon. Interpolated outgoing longwave radiation (OLR) (Liebmann and Smith, 1996) was used as a proxy for convective activities. The PERSIANN product has a horizontal resolution of 0.25×0.25 degrees, while the others have a resolution of 2.5×2.5 degrees.

To extract the ISO signals that might relate to the extreme rainfall event, the Lanczos bandpass filter (Duchon, 1979) is applied to the observed and reanalysis data. The active phase of the ISO of rainfall is determined by the period of at least three consecutive days when the bandpass-filtered rainfall has a positive value, and at least one day the filtered rainfall is greater than the climatological mean an amount of one standard deviation.

To evaluate the individual contribution of the synoptic-scale (3–10 day) variation, intra-seasonal (11–60 day) oscillation and long-term mean states (LTMS) to the extreme rainfall event, each columnwise anomalous moisture divergence is estimated as follows:

$$div(qv) \approx -\frac{1}{g} \int_{1000hPa}^{300hPa} \nabla \cdot \{(q_{3-10} + q_{11-60} + q_{mean})$$
$$(v_{3-10} + v_{11-60} + v_{mean})\}dp.$$

$$(1)$$

where p is the pressure, g is the gravitational acceleration, and (v_{3-10}, q_{3-10}), (v_{11-60}, q_{11-60}) and (v_{mean}, q_{mean}) are the wind and specific humidity of the 3–10-day oscillations, 11–60-day oscillations and LTMS components, respectively.
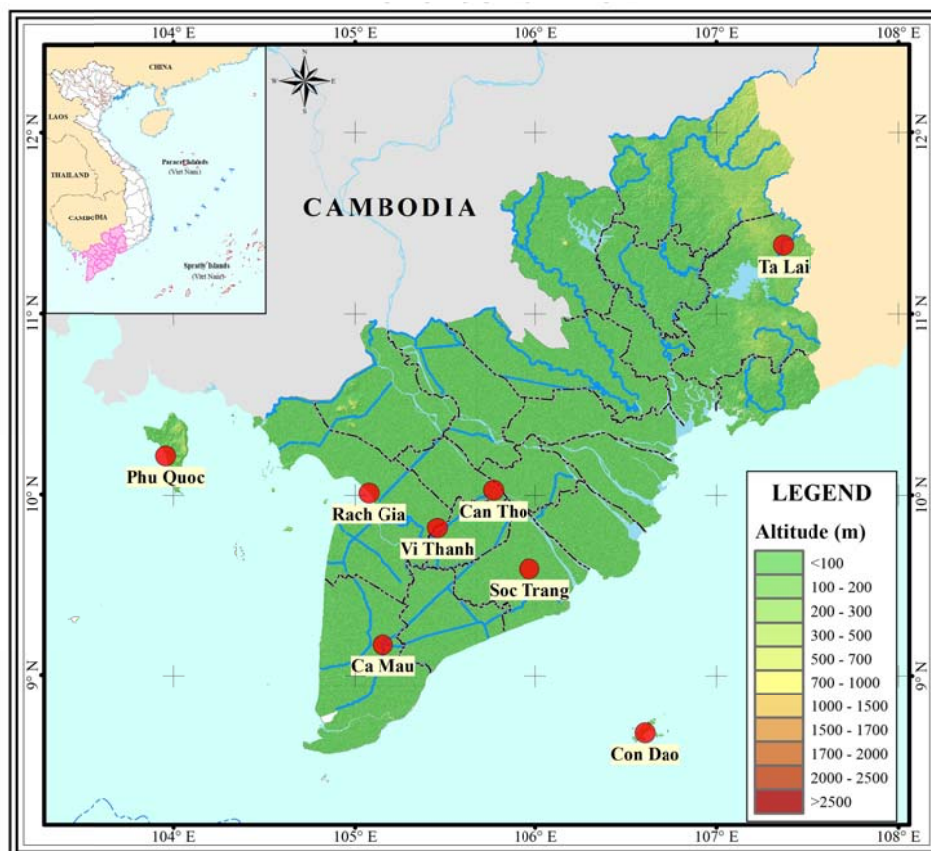
Figure 1. Topography (shaded, m) and selected rain gauges (red circles).

3. Results

3-1. Seasonal evolution of rainfall and large-scale circulation pattern

Rainfall over southern Vietnam shows strong seasonality (Thanh et al., 2010; Tuan, 2019). Figure 2 shows that in April, southern Vietnam is relatively dry due to the domination of the western North Pacific (WNP) subtropical high. However, in May, rainfall occurs over the southern plain, Cambodia and the BOB, concurrent with the eastward withdrawal of the subtropical high and the commencement of tropical westerlies over the Indian Ocean and the Indochina Peninsula (IP). Based on rainfall and zonal wind indices, Thanh et al. (2010) identified that the climatological onset date of the rainy season over the southern plain is approximately the 12th of May. This onset date agrees with other studies of summer monsoon onset over Vietnam and the IP (Matsumoto, 1997; Nguyen-Le et al., 2014). In the next three consecutive months, the Asian summer monsoon advances northward,

leading to widespread rainfall and strong zonal wind over a large monsoon region. This development of the monsoon westerlies also brings rich moisture from the BOB to IP and helps to maintain rainfall over the southern plain at a value of greater than 7 mm day^{-1} (see Figure appendix in the supplement to this article). After reaching the farthest north in August, the monsoon system gradually retreats in September, which is followed by a reduction in rainfall over the Indian Continent, BOB and Bien Dong. In contrast to these decreasing rainfall trends, rainfall in the southern plain reaches its highest peak in September (Thanh et al., 2010) due to modulations of multiple factors, including westerly monsoons, cold surges and tropical disturbances (Tuan, 2019; Nguyen-Thi et al., 2010; van der Linden et al., 2016). Finally, the rainy season over the southern plain ends in November with the dominance of northeast flows over the IP, which sets up unfavorable conditions for convection over the whole region.
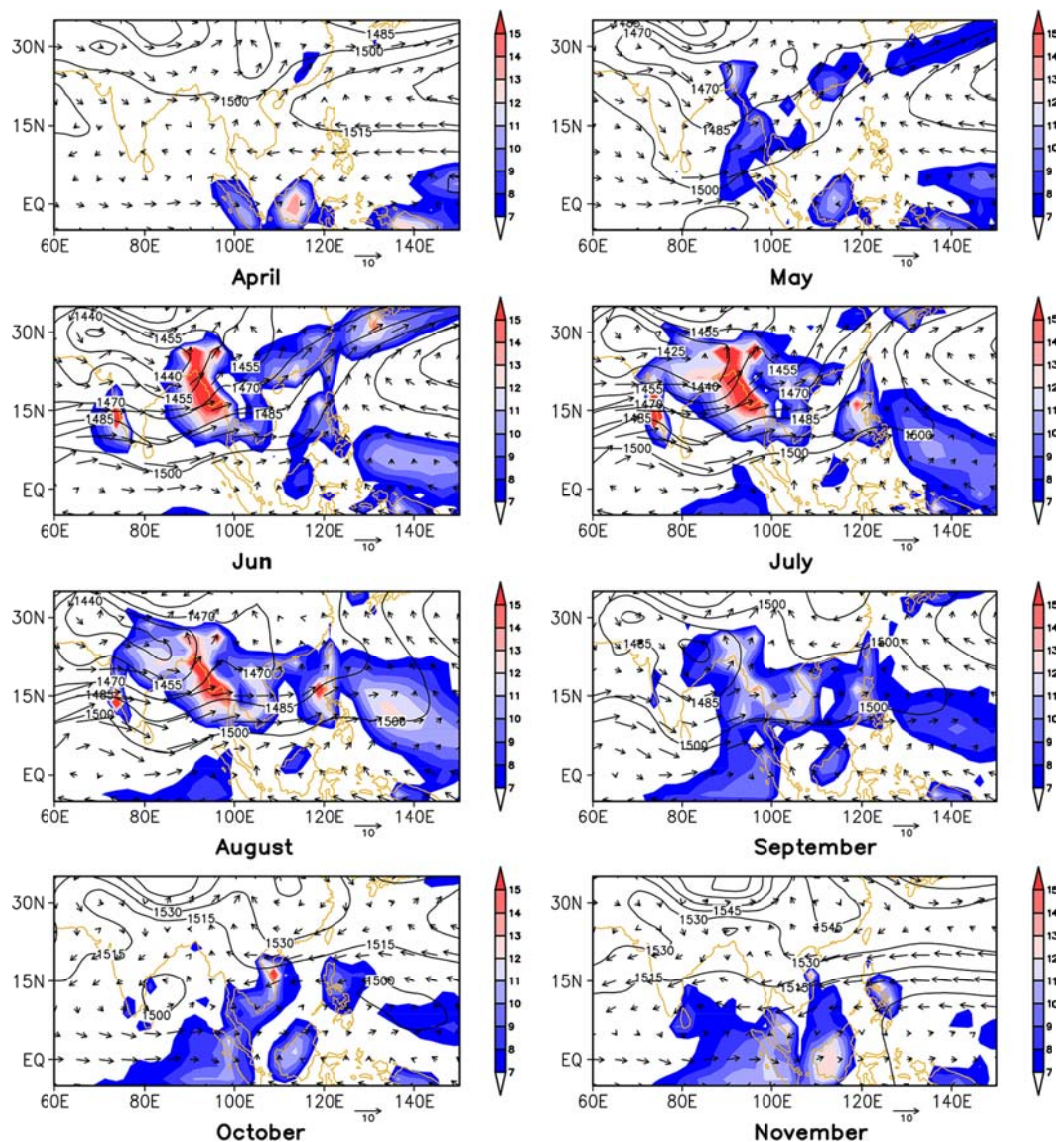
Figure 2. Climatological distribution of monthly mean wind (vector, m s^{-1}) and geopotential height (contour, m) at level of 850 hPa and GPCP data (shaded, mm day^{-1}) during 1981–2010.

3-2. Description of the extreme rainfall event

During August 1–15, 2019, long-lasting rainfall occurred over the southern plain, with a rainfall value first exceeding > 50 mm day^{-1} on August 2nd at some stations, such as Can Tho, Con Dao, Phu Quoc, Soc Trang, Rach Gia, and Vi Thanh. The rainfall then persisted for more than 10 days, with some rainfall peaks reaching > 100 mm day^{-1}, especially > 357.9 mm day^{-1} on August 9th at Phu Quoc station (Figure 3). For the period of 1980–2019, the peak of 357.9 mm day^{-1} was the second highest peak of the historical observed rainfall. The total rainfall in 15 days was > 1240.5 mm, which was the highest recorded rainfall for the 15-day period and accounted for approximately 45% of the climatology annual rainfall at that station. At almost all other stations, the total rainfall sum also reached high values, ranging from 80 mm to > 400 mm in those 15 days. The prolonged rainfall led to severe floods over much of the southern plain, especially in cities such as Ho Chi Minh, Can Tho, and Phu Quoc Island. Therefore, this event is considered an exceptional and extremely heavy rainfall event.

To identify the multiple-scale signals that might relate to the occurrence of the extreme rainfall event, the time evolutions of the 3–10-day and 11–60-day bandpass filters of the observed rainfall in the southern plain are plotted (Figure 3). Rainfall is strongly

modulated by synoptic-scale variations and ISOs, with rainfall peaks coinciding with the maxima of the two modes. Notably, the former consistently shows large fluctuations in the active phase of the latter. Especially from the second half of July to the first half of August, the ISO rainfall enters a strong active phase with a pronounced increase in its amplitudes. On Phu Quoc Island, the maximum low frequency amplitude is 10.4 times greater than its standard deviation in the 1980–2018

period. As expected, the maximum 3–10-day intensity also reaches as high as 15.1 times its standard deviation in the whole period. At other stations, the peaks of the ISOs and synoptic-scale variations also range from 3.1 to 6.3 and 2.1 to 6.1 times their standard deviations, respectively. In-phase developments of these two modes potentially intensified rainfall over the southern plain, especially on Phu Quoc Island, leading to record-breaking rainfall, as described earlier.
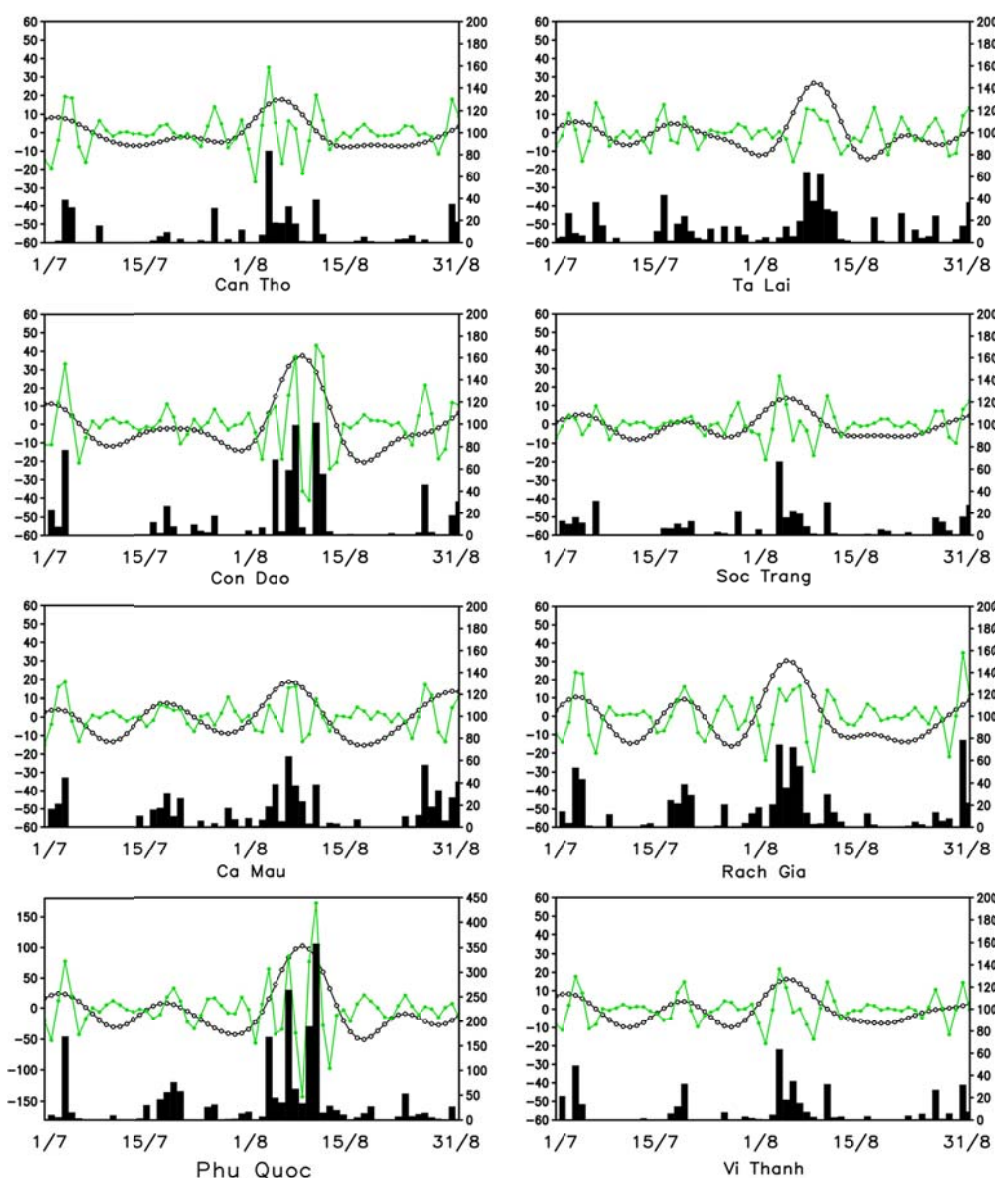

Figure 3. Observed rainfall (black bars, mm) and its 3–10-day (green dotted line, mm) and its 11–60-day bandpass filter (black dotted line, mm) for the period 1–15 August 2019 at the southern plain stations.

3-3. Evolution of large-scale circulation and convection

Figure 4 describes the time evolution of large-scale circulation and rainfall derived from PERSIANN satellite data during the extreme event in the southern plain. The pronounced noticeable signal is the strong intensification of westerlies in a large region from August 1–9. The high-value wind regions are embedded in a large zonal wind belt to the south of three cyclonic circulations north of the BOB, Bien Dong and the sea northeast of the Philippines. At the same time, a narrow rain band extends from the southern BOB to the south of Bien Dong, which is consistent with the rapid growth of the westerly flows. These patterns are consistent with our understanding of the interactions between low-level circulation and convection, which can be briefly explained as follows. Initially, the strong convective activities are closely associated with the maximum boundary layer convergences north of the maximum westerlies. However, the condensation latent heating released from convection generates westward-propagating Rossby waves, which accelerates the westerlies to the south and southwest of the maximum convection (Gill, 1980). As time passes, rainfall over India, the BOB and NWP show gradual propagations to the north, while the rain belt is still persistent over southern Vietnam, explaining the long-lasting occurrence of heavy rainfall in the sub-region.
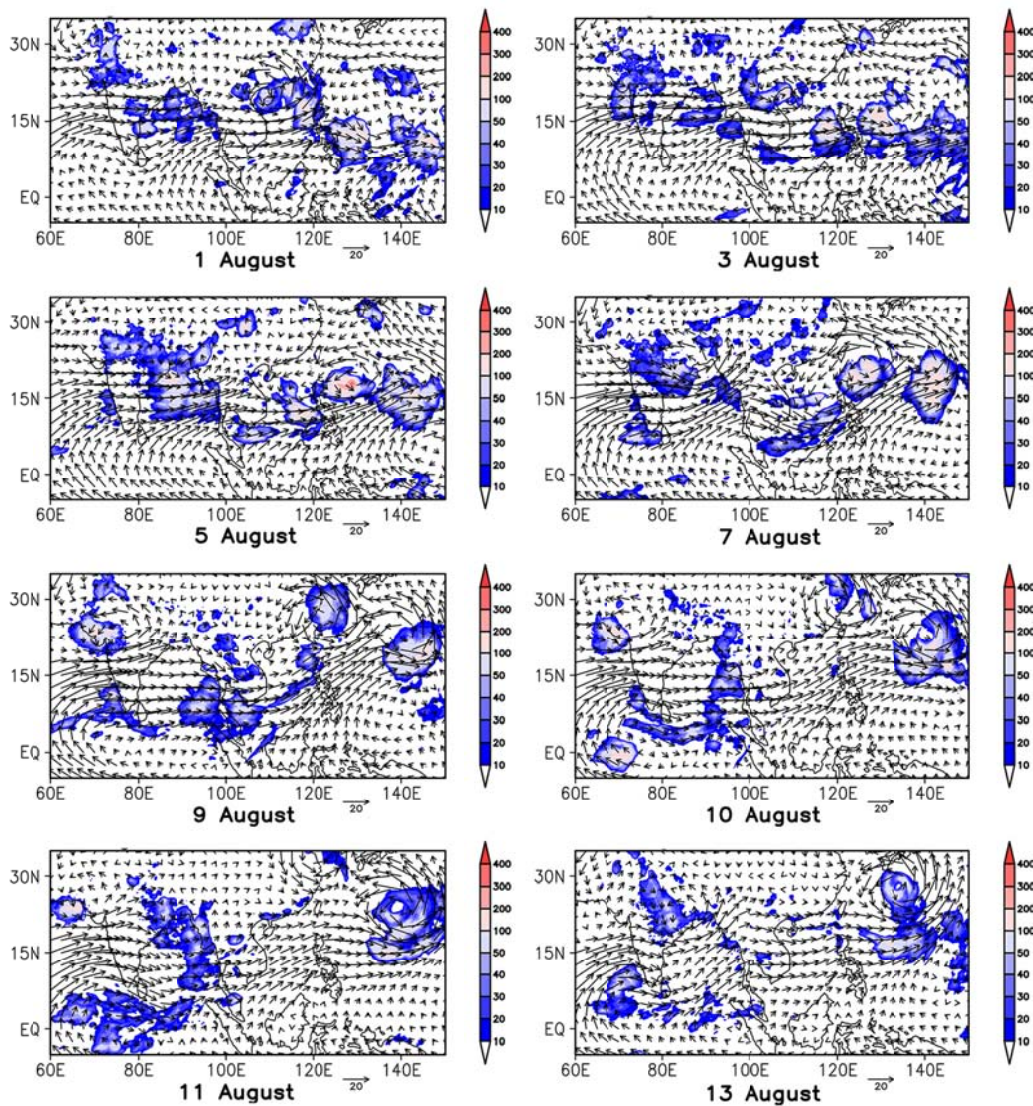
Figure 4. Evolution of 850 hPa wind (vector, m s^{-1}) and PERSIAAN rainfall data (shaded, mm) for the period 1–13 August 2019.

From August 1 to 5, a clear signal can be noticed in the 11–60-day mode because of the existence of a series of large-scale cyclonic anomalies over the WNP and the northern BOB (Figure 5). The southeast–northwest orientations of the anomalous cyclones and negative OLR are reminiscent of the structure of the boreal summer ISO (BSISO) over the WNP region (Murakami, 1984; Kemball-Cook and Wang, 2001). The southern plain is under the control of strengthening westerlies associated with active convection south of these cyclones. Thus, the 11–60-day oscillation provides a favorable background to supply rich moisture from the BOB to the southern plain. As the ISO rainfall reaches its mature phase and then transitions to the break phase, these cyclonic anomalies over the WNP gradually move northward and are subsequently replaced by a series of anti-cyclonic circulations. This phenomenon occurs concurrently with the change from cyclonic to anti-cyclonic anomalies over the north of the BOB. As a result, the southern plain is exposed to anomalous south-easterlies associated with suppressed convection.

During that period, the evolution of the 3–10-day mode is characterized by more complex movements of a series of synoptic-scale disturbances over the WNP region (Figure 6). On August 1–5, two wave trains are observed, with the stronger at approximately 120°E–160°E, 12°N–25°N (denoted as A1-C1-A2-C2) and the weaker at approximately 100°E–140°E, 0–15°N (denoted as A1-C1-A2-C2). On the following days, while the stronger wave train propagates northwestward and heads to the East China Sea, the weaker wave train deepens rapidly and then crosses the southern plain.
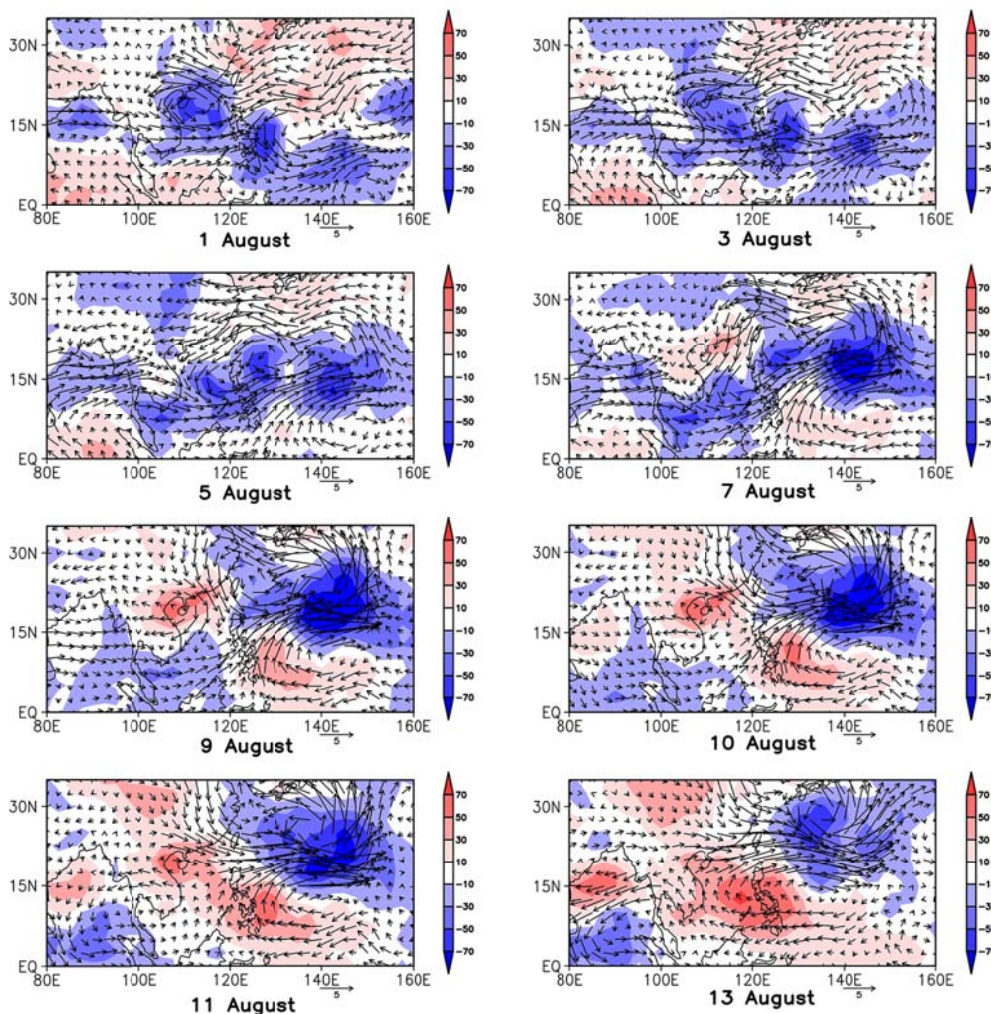

Figure 5. 11–60-day bandpass filter of 850-hPa wind (*vector*, m s^{-1}) and OLR (*shaded*, m s^{-1}) for the period 1–13 August 2019.

It is important to note that this intensification of the wave train is concurrent with the sharp increase of the ISO amplitude. As a result, the southern plain is under the control of deep convection south of the cyclonic anomaly on August 7–9.

3-4. Scale interactions

As addressed by previous studies, low-frequency background flows provide a favorable environment for higher-frequency activities (Liblmann et al., 1994, Hsu et al., 2011, Straub and Kiladis, 2003). By diagnosing the different terms of the perturbation eddy kinetic energy equation, Hsu et al. (2011) reported that while the LTMS over the WNP always supplies energy for synoptic-scale eddies to develop, the ISO helps to intensify the eddies in the active phase and suppress them in the break phase.

The rainfall data for the whole period of 1980-2019 also indicate that the 3–10-day mode of average rainfall over the southern plain tends to be significantly enhanced when the 11–60-day oscillation displays its high amplitudes. There were 40 occasions in which the 3–10-day oscillation intensity exceeded 4 standard deviations when the 11–60-day oscillation amplitude was greater than 2 standard deviations. These occasions comprise 82.35% of the total cases where the 3–10-day intensity exceeded 4 standard deviations. The criteria of 2 and 4 standard deviations are chosen to emphasize the strong amplitude of the oscillations. The data also indicate that the rainfall on the southern plain stations always shows extreme values when the two modes concurrently are greater than their aforementioned critical positive values.
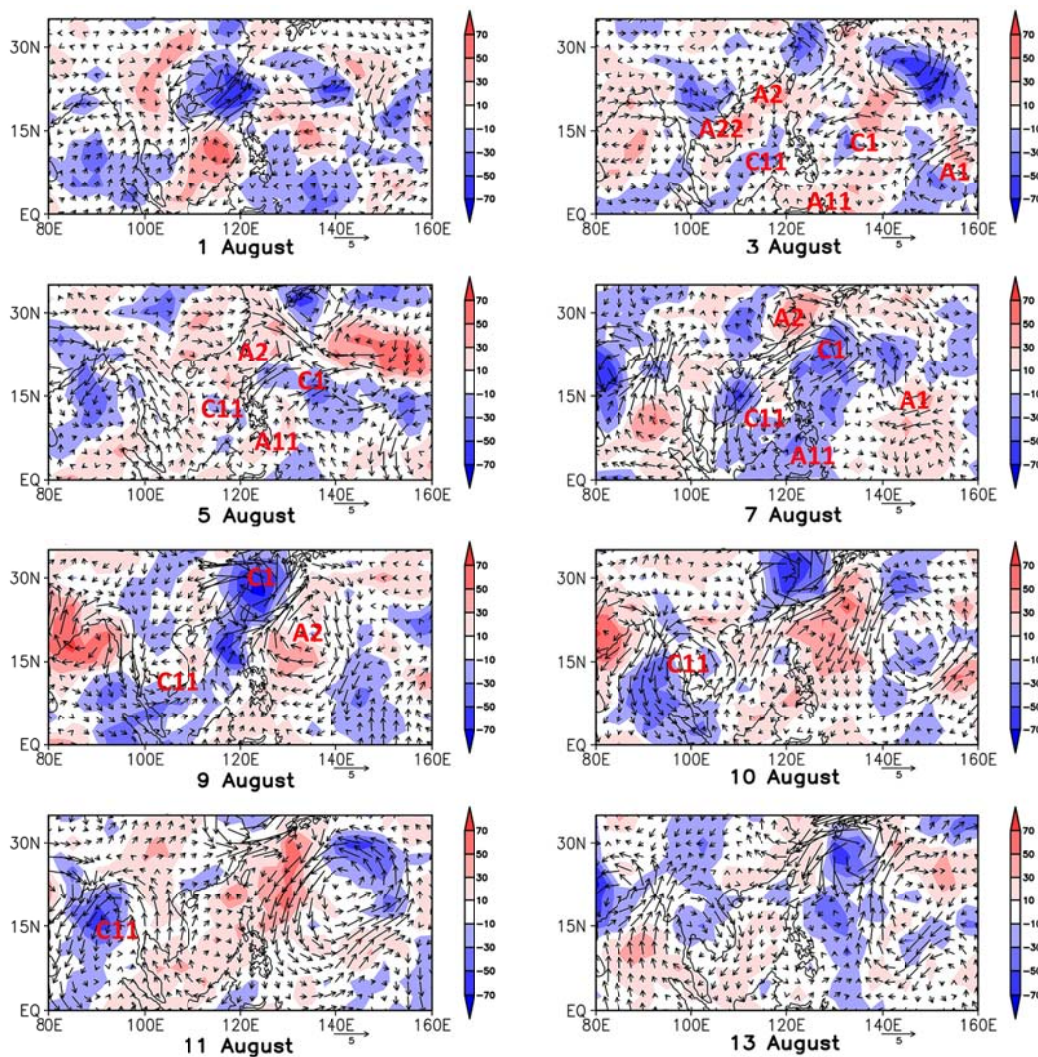
Figure 6. The same as Figure 3, except for 3–10-day bandpass filter. The A1, A2, A11, A22 denote the anomalous anti-cyclones and C1, C11 denote the anomalous cyclones.

While the relationship between the sub-monthly oscillation and the occurrence of heavy rainfall in the southern plain is not very clear (Tuan, 2019), the obtained result suggests that the mutual interactions of the 3–10-day variation, 11–60-day oscillations and LTMS are almost certainly the major cause of extreme rainfall in the sub-region.

To elaborate on that argument, the effects of the synoptic-scale variation, ISO and LTMS are estimated (Figure 7). The similar pattern of the total columnwise moisture divergence to the sum of the anomalous vertical moisture divergence terms indicates that the former can be approximately estimated by the latter. There are two significant negative anomalous moisture divergences that match the occurrence of heavy rainfall in the southern plain. These negative anomalous moisture divergences are even smaller than the total moisture divergences. This pattern shows that heavy rainfall is mostly induced by the mutual interaction of the synoptic-scale variation, ISO and LTMS. For more details, on August 5th, the low frequency convergence and synoptic-scale moisture variation, the synoptic-scale moisture transported by the long-term mean flow and the low frequency convergence of the long-term mean of moisture show dramatic drops, emphasizing their important roles in inducing heavy rainfall. Similarly, synoptic-scale convergence of the long-term mean moisture and the low frequency moisture transported by the long-term mean flow are considered the two largest contributors that lead to the heavy rainfall on August 9th.
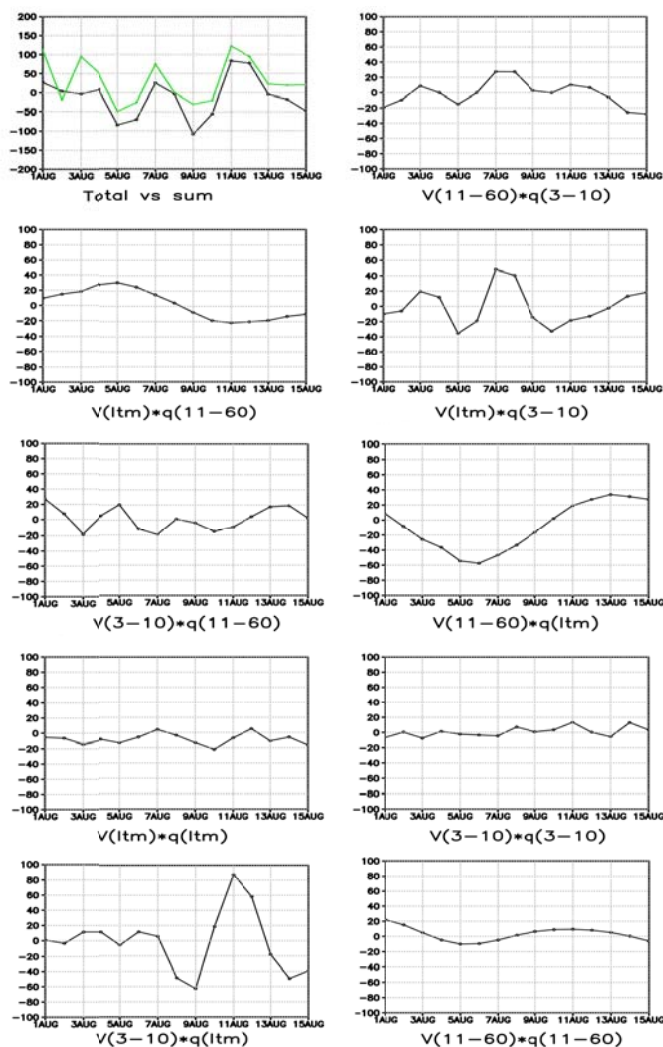
Figure 7. Average of total vertically moisture divergence (green line) and sum of anomalous vertically moisture divergence terms (black line) (a) and individual anomalous vertically moisture divergence terms (black line) (b–j) over the southern plain (105°E –108°E, 8°N –12°N). Unit is 10^{-7} kg m^{-2} s^{-1}. V and q are wind (m s^{-1}) and specific humidity (kg kg^{-1}) respectively.

4. Discussion

Most tropical rainfall is produced by organized convective systems involving processes that occur on multiple spatial and temporal scales. Though the high stochastic activity of convection limits the accurate forecast of numerical weather prediction systems, a better understanding of how large-scale environments induce extreme rainfall can raise the predictability of regional forecasts. In the Indian and East Asian monsoon regions, the MJO and BSISO are two dominant modes of the ISO; thus, they have been considered major sources of extreme rainfall predictability (Xavier et al., 2014; Wang and Moon, 2017; Lee et al., 2017). Based on the relationship between extreme rainfall and BSISO activity, Lee et al. (2017) noted that the prediction of extreme rainfall over Asia on a subseasonal time scale is promising. Vietnam lies in the transition zone of the Indian and East Asian summer monsoon systems, and the relation between extreme rainfall events and the ISO in Vietnam was also addressed in previous studies (Tuan, 2019; van der Linden et al., 2016; Chen et al., 2012; Wu et al., 2011; Yokoi and Matsumoto, 2008). While past studies investigated synoptic development related to individual extreme rainfall cases (Chen et al., 2012b; Wu et al., 2011; Yokoi and Matsumoto, 2008), others focused on estimating the probability of extreme rainfall in the ISO phases (van der Linden et al., 2016; Tuan, 2019). However, few methodologies have been adopted to utilize these previous results in real-time heavy rainfall forecasts in Vietnam. As far as the authors are aware, the study by Chen et al. (2020a) is the only one that developed a forecast advisory for 1-week heavy rainfall prediction in Central Vietnam.

The present study explored the collective influences of the LTMS, BSISO and other higher frequency oscillations on the occurrence of an extreme rainfall event over southern Vietnam. The statistics also show that the probability of heavy rainfall in the southern plain increases in the wet phase of BSISO. However, it is important to note that there is significant day-to-day variability of heavy rainfall in that phase because of modulations of other scale processes. The results suggest using multiple indices to predict extreme rainfall instead of one BSISO index as proposed by Lee et al. (2017). It is expected that the combination of information from multiple processes will help to improve the ability of capturing extreme rainfall occurrence and intensity at the subseasonal scale. Constructing the new indices and testing their feasibility in real-time extreme rainfall forecasts in southern Vietnam are important areas for future studies.

5. Conclusion

This study investigated the characteristics of large-scale patterns associated with the extreme rainfall event in southern Vietnam during August 1–15, 2019, using data from rain gauges, OLR and NCEP/NCAR re-analyses. The results show significant intensifications of both 3–10-day and 11–60-day modes during the event. The development of the ISO is characterized by the northeastward propagation of a series of cyclonic anomalies over the WNP and the replacement of a cyclonic anomaly by an anti-cyclonic anomaly over the north of the BOB. The representation of anomalous cyclones over the WNP to the East China Sea and the IP are important synoptic-scale variations for the heavy rainfall event. The anomalous convergences and the synoptic-scale moisture transported by the mean flow are important factors for occurrence of the heavy rainfall event in the southern plain region.

Fangchenggang nuclear power plants to Vietnam".

References

Adler, R.F., Sapiano, M.R.P., Huffman, G.J., Wang, J.-J., Gu, G., Bolvin, D., Chiu, L., Schneider, U., Becker, A., Nelkin, E., Xie, P., Ferraro, R. and Shin, D.-B., 2018, The Global Precipitation Climatology Project (GPCP) Monthly Analysis (New Version 2.3) and a Review of 2017 Global Precipitation. Atmosphere 2018, 9, 138.

Chen, T., Yen, M., Tsay, J., Alpert, J. and Tan Thanh, N. T., 2012, Forecast Advisory for the Late Fall Heavy Rainfall/Flood Event in Central Vietnam Developed from Diagnostic Analysis. Wea. Forecasting, 27, 1155–1177.

Chen, T., Yen, M., Tsay, J., Tan Thanh, N. T. and Alpert, J., 2012, Synoptic Development of the Hanoi Heavy Rainfall Event of 30–31 October 2008: Multiple-Scale Processes. Mon. Wea. Rev., 140, 1219–1240.

Duchon, C.E., 1979, Lanczos Filtering in One and Two Dimensions. J. Appl. Meteor., 18, 1016–1022.

Gill, A.E., 1980, Some simple solutions for heat-induced tropical circulation. Q. J. R. Meteorol. Soc., 106(449), 447-462.

Hsu, P., Li, T. and Tsou, C., 2011, Interactions between Boreal Summer Intraseasonal Oscillations and Synoptic-Scale Disturbances over the Western North Pacific. Part I: Energetics Diagnosis. J. Climate., 24, 927–941.

Kalnay, E., Kanamitsu, M., Kistler, R., Collins, W., Deaven, D., Gandin, L., Iredell, M., Saha, S., White, G., Woollen, J., Zhu, Y., Chelliah, M., Ebisuzaki, W., Higgins, W., Janowiak, J., Mo, K.C., Ropelewski, C., Wang, J., Leetmaa, A., Reynolds, R., Jenne, R. and Joseph, D., 1996, The NCEP/NCAR 40-Year Reanalysis Project. Bull. Amer. Meteor. Soc., 77,437–472.

Kemball-Cook S., Wang, B., 2001, Equatorial waves and air-sea interaction in the boreal summer intraseasonal oscillation. J. Clim., 14, 2923–2942.

Lee, S. S., Moon, J. Y., Wang, B. and Kim, H. J., 2017, Subseasonal prediction of extreme precipitation over Asia: Boreal summer intraseasonal oscillation perspective. J. Climate, 30(8), 2849-2865.

Liebmann, B. and Smith, C.A., 1996, Description of a Complete (Interpolated) Outgoing Longwave Radiation Dataset. Bulletin of the American Meteorological Society, 77, 1275-1277.

Matsumoto, J., 1997, Seasonal transition of summer rainy season over Indochina and adjacent monsoon region. Adv. Atmos. Sci., 14, 231–245.

Murakami, M., 1984, Analysis of deep convective activity over the western Pacific and southeast Asia. Part II: seasonal and intraseasonal variations during northern summer. J. Meteorol. Soc. Jpn., 62, 88–108.

Nguyen, D.N. and Nguyen, T.H., 2004, Climate and climate resource of Vietnam. Agricultural Publishing House.

Nguyen, D.Q., Renwick, J. and McGregor, J., 2014, Variations of surface temperature and rainfall in Vietnam from 1971 to 2010. Int. J. Climatol., 34, 249-264.

Nguyen, P., Shearer, E.J., Tran, H., Ombadi, M., Hayatbini, N., Palacios, T., Huynh, P., Updegraff, G., Hsu, K., Kuligowski, B., Logan, W.S. and Sorooshian, S., 2019, The CHRS Data Portal, an easily accessible public repository for PERSIANN global satellite precipitation data, Nature Scientific Data, 6, Article 180296.

Nguyen-Le, D., Matsumoto, J. and Ngo-Duc, T., 2014, Climatological onset date of summer monsoon in Vietnam. Int. J. Climatol., 34: 3237-3250.

Nguyen-Thi, H.A., Matsumoto, J., Ngo-Duc, T. and Endo, N., 2012, A climatological study of tropical cyclone rainfall in Vietnam. Sola, 8, 41-44.

Pham, X.T., Fontaine, B. and Philippon, N., 2010, Onset of the summer monsoon over the southern Vietnam and its predictability. Theor Appl Climatol 99, 105–113.

Straub, K.H. and Kiladis, G.N., 2003, Interactions between the Boreal Summer Intraseasonal Oscillation and Higher-Frequency Tropical Wave Activity. Mon. Wea. Rev., 131, 945–960.

Takahashi, H. G., Fujinami, H., Yasunari, T., and Matsumoto, J., 2010, Diurnal rainfall pattern observed by Tropical Rainfall Measuring Mission Precipitation Radar (TRMM-PR) around the Indochina

peninsula. J. GEOPHYS. RES-ATMOS., 115(D7).

Tuan, B.M., 2019, Extratropical Forcing of Submonthly Variations of Rainfall in Vietnam. J. Climate, 32, 2329–2348.

Van der Linden, R., Fink, A.H., Pinto, J.G., Phan-Van, T. and Kiladis, G.N., 2016, Modulation of Daily Rainfall in Southern Vietnam by the Madden–Julian Oscillation and Convectively Coupled Equatorial Waves. J. Climate, 29, 5801–5820.

Wang, B. and Moon, J. Y., 2017, Subseasonal prediction of extreme weather events. Bridging Science and Policy Implication for Managing Climate Extremes: Linking Science and Policy Implication.

Wu, P., Fukutomi, Y. and Matsumoto, J., 2011, An observational study of the extremely heavy rain event in northern Vietnam during 30 October-1 November 2008. J. Meteorol. Soc. Japan. Ser. II, 89, 331-344.

Xavier, P., Rahmat, R., Cheong, W.K. and Wallace, E., 2014, Influence of Madden–Julian oscillation on Southeast Asia rainfall extremes: Observations and predictability. Geophys. Res. Lett., 41, 4406–4412.

Yasunaga, K., and Mapes, B., 2012, Differences between more divergent and more rotational types of convectively coupled equatorial waves. Part II: Composite analysis based on space–time filtering. J. Atmos. Sci., 69, 17–34.

Yokoi, S. and Matsumoto, J., 2008, Collaborative effects of cold surge and tropical depression–type disturbance on heavy rainfall in central Vietnam. Mon. Wea. Rev., 136(9), 3275-3287.

Vietnmnew, 2019, Phú Quốc needs answers after historic floods. (Available online at: https://vietnamnews.vn/society/523872/phu-quoc-needs-answers-after-historic-floods.html).

Appendix (Supplemental material)
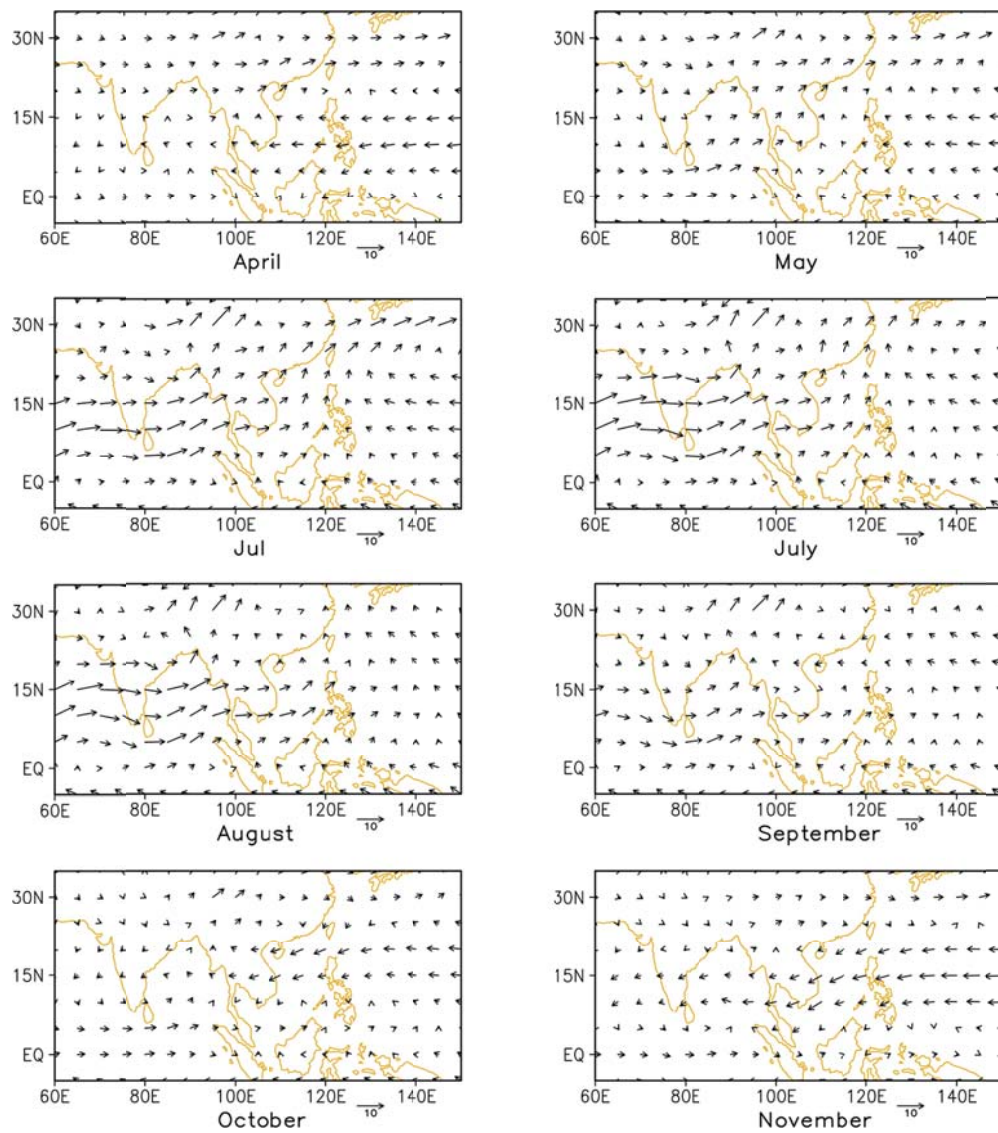
Figure. Climatological distribution of monthly mean of total vertically moisture flux (*vector*) during 1981-2010. Unit is 10-7 kg m-2 s-1